



**HAL**  
open science

## **Carbon screen-printed electrodes modified by a polycatechol film for Cu and Pb detection in acidified drinking water**

Corinne Parat, Estelle Ricard, Wahid Ben Mefteh, Isabelle Le Hécho

### ► **To cite this version:**

Corinne Parat, Estelle Ricard, Wahid Ben Mefteh, Isabelle Le Hécho. Carbon screen-printed electrodes modified by a polycatechol film for Cu and Pb detection in acidified drinking water. *Electrochimica Acta*, 2023, 461, pp.142666. <10.1016/j.electacta.2023.142666>. <hal-04142593>

**HAL Id: hal-04142593**

**<https://univ-pau.hal.science/hal-04142593v1>**

Submitted on 27 Jun 2023

**HAL** is a multi-disciplinary open access archive for the deposit and dissemination of scientific research documents, whether they are published or not. The documents may come from teaching and research institutions in France or abroad, or from public or private research centers.

L'archive ouverte pluridisciplinaire **HAL**, est destinée au dépôt et à la diffusion de documents scientifiques de niveau recherche, publiés ou non, émanant des établissements d'enseignement et de recherche français ou étrangers, des laboratoires publics ou privés.



HAL Authorization

# Carbon screen-printed electrodes modified by a polycatechol film for Cu and Pb detection in acidified drinking water

Corinne Parat\*, Estelle Ricard, Wahid Ben Mefteh, Isabelle Le Hécho

CNRS / Univ Pau & Pays Adour / E2S UPPA, Institut des sciences analytiques pour l'environnement et les matériaux, UMR5254, 2 avenue Pierre Angot, 64000 Pau, France

\*corresponding author: [corinne.parat@univ-pau.fr](mailto:corinne.parat@univ-pau.fr)

## Abstract

The dissolution of metals such as Cu or Pb in water can be increased by prolonged stagnation of water in internal pipes of drinking water networks, resulting in high concentrations in the consumer's tap water. As they can accumulate in biota and affect living organisms with more or less serious long-term toxic effects, the monitoring of Cu or Pb in tap water and more generally in aquatic environments is therefore an important issue. For this purpose, a new electrochemical sensor based on a screen-printed carbon electrode modified with a polycatechol film was developed for the highly sensitive detection of Cu and Pb in drinking water. The electropolymerisation was first optimised to obtain a homogeneous and reproducible film for the detection of trace metals. The mechanism of the polymerization process was proposed and discussed. Then, the performance of the new sensor was evaluated. The pH and the conductivity were found to be the main parameters influencing the sensitivity of the sensors. Thus, the electrochemical analyses carried out at pH values around neutrality with this device made it possible to determine the free and labile forms of metal in solution, while the total metal contents were determined after acidification of water samples to pH 5 or less. Furthermore, a stable signal was obtained from  $470 \mu\text{S cm}^{-1}$ , which means that most of freshwater rivers and mineral waters can be directly analysed without any supporting electrolyte addition. After optimisation of the analytical conditions, a

30 sensitivity of the order of  $\mu\text{g L}^{-1}$  was reached for a deposition time of 60 s while an  
31 electrodeposition time of 300 s gave a sensitivity of  $\text{ng L}^{-1}$ .

32

33 **Keywords:** Electropolymerisation, *in situ* detection, trace metals, stripping  
34 chronopotentiometry

35

36

## 37 **1. Introduction**

38 The presence of metals such as lead (Pb) and copper (Cu) in water leaving water  
39 production facilities is low or undetectable. However, these substances can be found in  
40 higher concentrations in the consumer's tap water due to the dissolution of these metals  
41 in the water contained in the pipes (internal networks and possibly public connections),  
42 valves and fittings of the internal networks of buildings [1]. Concentrations in drinking  
43 water vary from 0.005 to 30 mg/L for Cu, mainly due to corrosion in internal Cu pipes,  
44 and are generally below 5  $\mu\text{g/L}$  for Pb, although much higher concentrations (above 100  
45  $\mu\text{g/L}$ ) have been measured in the presence of Pb pipes or fittings [2]. While there is still  
46 some uncertainty regarding the long-term effects of copper on sensitive populations [3], this is  
47 not the case of Pb which is recognized as a chemical of high public health concern.  
48 Thus, the quality limit in water intended for human consumption is currently set at 10  
49  $\mu\text{g/L}$  for Pb and at 2 mg/L for Cu by Directive 2020/2184 in accordance with the guide  
50 value recommended by the World Health Organisation (WHO) [4].

51 According to WHO, exposure must be assessed using an appropriate sampling strategy,  
52 taking into account when, where, and how samples are collected, as well as the number  
53 of samples to be collected [5]. Monitoring of metals in tap water and more generally in  
54 aquatic environments is therefore an important issue as they can accumulate in the biota  
55 and affect living organisms with more or less serious long-term toxic effects [6, 7].  
56 Among the available analytical techniques, only a few approaches allow the  
57 implementation of suitable *in situ* devices in terms of analytical performance,  
58 autonomy, miniaturization feasibility, and ease of transport [8]. Due to their high  
59 sensitivity, electrochemical techniques, such as anodic stripping voltammetry (ASV)  
60 and stripping chronopotentiometry (SCP) using disposable sensors, have proven to be  
61 promising approaches for the analysis of metals in freshwater [9-14]. Among one single-

62 use sensors, screen-printed electrodes have been increasingly studied due to their  
63 performance and ability to be mass-produced at very low costs [15-18]. In addition,  
64 their surface can be easily modified, which has led to different improvements in the  
65 final sensor, such as increased selectivity and/or sensitivity. Most screen-printed sensors  
66 for sensitive determination of metals were based on a mercury film as a modifier of the  
67 working surface [19-21]. Due to the toxicity of mercury, several new types of mercury-  
68 free film electrodes have been developed for trace metal detection, such as bismuth-  
69 coated carbon electrodes [22-24] or gold-film electrodes [25-28]. Recent achievements  
70 show the electrochemical detection of trace metals with electrodes modified with  
71 inorganic, organic and biological materials [29-31]. Metal, metal oxide, carbon and  
72 silica-based nanomaterials have emerged as the most commonly used nanomaterials for  
73 electrochemical detection of trace metals [17, 32, 33]. Organic polymers have also been  
74 widely employed in sensor construction [34, 35]. Polyaniline, polypyrrole and poly(3,4-  
75 ethylenedioxythiophene) are the main conductive polymers used for biosensors due to  
76 their low-cost synthesis, high sensitivity, and excellent stability [36]. Catechol is a  
77 simple molecule, capable of establishing a wide range of interactions with organic and  
78 inorganic analytes [37, 38]. Depending on the pH, it also showed a tendency to form  
79 mono-, di-, or tri-coordinated complexes with metals like Cu, Zn, Ni, Co, Mn, Fe [39-  
80 42]. Thus, Koo *et al* demonstrated that a polycatechol film deposited on a glassy carbon  
81 electrode allowed the preconcentration of Ce(III) before its detection by differential  
82 pulse anodic stripping voltammetry [43].

83 All these works suggest that polycatechol is a good candidate for the development of an  
84 electrochemical sensor for *in situ* trace metal detection. The present study focused on  
85 the original development of an electrochemical sensor for Cu and Pb monitoring in  
86 drinking water. Our objective was to modify the working surface of a screen-printed  
87 electrode by a polycatechol film in order to form a time-stable, low-cost, robust and  
88 sensitive electrochemical platform for a direct metal detection in a freshwater sample.  
89 After optimizing the electrodeposition of the polycatechol film on a carbon-based  
90 screen-printed electrode (SPCE), the performance of the modified sensor for Cu and Pb  
91 detection was investigated and then tested in a mineral water sample.

92

## 93 **2. Experimental**

### 94 **2.1 Chemicals and reagents**

95 The polystyrene support for the screen printing was obtained from Sericol. The  
96 commercial ink (electrodag PF-407A) was purchased from Acheson Colloids. Acetic  
97 acid ( $\text{CH}_3\text{COOH}$ , Trace select), sodium acetate trihydrate ( $\text{CH}_3\text{COONa}$ , Trace select)  
98 were obtained from Fluka. Nitric acid (69-70%, Baker Instra-Analysed for trace metal  
99 analysis) and sodium hydroxide (Baker Analysed) were obtained from J.T. Baker.  
100 Mesitylen, disodium hydrogen phosphate dihydrate ( $\text{Na}_2\text{HPO}_4 \cdot \text{H}_2\text{O}$ ), sodium phosphate  
101 monobasic ( $\text{NaH}_2\text{PO}_4$ ) and 1,2-dihydroxybenzene (catechol) were purchased from  
102 Sigma-Aldrich. The stock solutions at  $1000 \text{ mg L}^{-1}$  of Cu and Pb were obtained from  
103 Merck. Ultrapure water (resistivity of  $18 \text{ M}\Omega \text{ cm}$ ) was used for dilutions. Acetate buffer  
104 solution ( $0.1 \text{ mol L}^{-1}$ , pH 4.6) was prepared by mixing appropriate amounts of  
105  $\text{CH}_3\text{COOH}$  and  $\text{CH}_3\text{COONa}$ . Phosphate buffer ( $0.1 \text{ mol L}^{-1}$ , pH 7.5) was prepared by  
106 mixing appropriate amounts of  $\text{Na}_2\text{HPO}_4$  and  $\text{NaH}_2\text{PO}_4$ . Chemical composition of the  
107 mineral water was: calcium  $68 \text{ mg L}^{-1}$ , potassium  $11 \text{ mg L}^{-1}$ , magnesium  $2 \text{ mg L}^{-1}$ ,  
108 sodium  $21 \text{ mg L}^{-1}$ , bicarbonates  $219 \text{ mg L}^{-1}$ , chlorides  $28 \text{ mg L}^{-1}$ , sulphates  $39 \text{ mg L}^{-1}$ ,  
109 nitrates  $1 \text{ mg L}^{-1}$ , pH 7.6, conductivity  $476 \mu\text{S cm}^{-1}$  (equivalent to  $285 \text{ mg L}^{-1}$ ).

110

## 111 **2.2 Instruments**

112 All electrochemical measurements were performed on an Eco Chemie  $\mu\text{Autolab III}$   
113 connected to a Metrohm 663 VA Stand and a computer using the GPES 4.9 software  
114 package (Eco Chemie). Electrochemical measurements were performed by means of a  
115 three electrode-system: a screen-printed carbon electrode (SPCE) with an active area of  
116  $9.6 \text{ mm}^2$  as working electrode, a carbon auxiliary electrode and an Ag/AgCl KCl ( $3 \text{ mol}$   
117  $\text{L}^{-1}$ ) reference electrode encased in a  $0.1 \text{ mol L}^{-1}$   $\text{KNO}_3$  jacket. A 3mm diameter glassy  
118 carbon electrode (GCE) from Syclope Electronique was also tested as a working  
119 electrode.

120

## 121 **2.3 Preparation of catechol modified screen-printed electrode**

122 The electrodes were manually screen printed on 1 mm-thick polystyrene plates using a  
123 commercial carbon-based ink to produce a set of 8 electrodes (Figure S1) [10]. After a  
124 drying step (1 hour at room temperature) and a curing step (1 hour in an oven at  $60^\circ\text{C}$ ),  
125 an insulating layer (polystyrene dissolved in an adequate volume of mesitylene) was  
126 manually spread over the conductive track, leaving a working disk area of  $9.6 \text{ mm}^2$  and  
127 an electrical contact.

128 The electrodeposition of catechol (1,2-Dihydroxybenzene) on the SPCE working  
129 surface was carried out in three steps. The following conditions correspond to the  
130 optimised conditions. The first step was the electrodeposition of catechol ( $10 \text{ mmol L}^{-1}$ )  
131 on the working surface by cyclic voltammetry (CV) between  $-0.8 \text{ V}$  and  $+0.8 \text{ V}$  versus  
132 Ag/AgCl at scan rate of  $200 \text{ mV s}^{-1}$  in phosphate buffer (pH 7.2). The modified  
133 electrode was characterized by CV at  $200 \text{ mV s}^{-1}$ , using a monomer-free acetate buffer  
134 solution (pH 4.8). In a second step, the electrode was rinsed with water, immersed in  $0.1$   
135  $\text{mol L}^{-1}$  NaOH and cycled until a stable baseline was obtained. The final step was to air  
136 dry for 24 hours. The sensor is stored in the open air when not in use.

137

## 138 **2.4 Electrochemical measurements**

139 Trace metal measurements were performed at room temperature in a  $0.1 \text{ mol L}^{-1}$  acetate  
140 supporting electrolyte at pH 4.8 by SCP. Like the usual stripping voltammetry  
141 techniques, SCP requires two steps: a deposition (accumulation) step in which metal  
142 ions are reduced at a constant potential, followed by a stripping (quantification) step  
143 involving reoxidation by applying a constant oxidising current. The analytical signal is  
144 the time required for reoxidation (transition time  $\tau$ ). A reliable determination of  $\tau$  is  
145 obtained by measuring the area under the peak in the  $dt/dE$  versus  $E$  plot, where  $dt/dE$  is  
146 the inverse of the time ( $t$ ) derivative of the recorded potential ( $E$ ) [44, 45]. After  
147 optimisation, the analytical parameters were as follows: an electrodeposition step of 60  
148 s at  $-1.2 \text{ V}$  with stirring, followed by an equilibration time of 10 s at  $-1.2 \text{ V}$  without  
149 stirring and a stripping step by applying a stripping current ( $I_s$ ) of  $10 \text{ }\mu\text{A}$  without  
150 stirring.

151

## 152 **2.5 Analytical performance**

153 Analytical performance (sensitivity, limit of detection and limit of quantification) of the  
154 modified SPCE was investigated using SCP, an analytical technique that allows the  
155 detection of trace metals at low concentrations (in the  $\mu\text{g L}^{-1}$  range) by applying the  
156 electrochemical parameters described above. Analyses were performed without purging  
157 at room temperature in a  $0.1 \text{ mol L}^{-1}$  acetate supporting electrolyte at pH 4.6, doped in  
158 Cu or Pb. Validation of the sensor was performed by SCP in a mineral water acidified at  
159 pH 4.6 with acetic acid, and doped in Cu at  $40 \text{ }\mu\text{g L}^{-1}$  in order to determine the total Cu  
160 concentration.

161

## 162 **2.6 Statistical approach**

163 The reliability of the sensor manufacture was based on the reproducibility, which was  
164 investigated by first comparing 8 modified SPEs from the same screen-printing plate  
165 (intra-plate reproducibility) and then by comparing 8 modified SPCEs from 8 different  
166 screen-printing plates (inter-plate reproducibility) (Figure S1). For each sensor, the  
167 mean Cu signal and its standard deviation, based on three replicates, were determined  
168 for a Cu concentration of 20  $\mu\text{g L}^{-1}$  in a 0.1 mol  $\text{L}^{-1}$  acetate buffer.

169 The linearity and the sensitivity were obtained from the calibration plot based on 3  
170 replicate analyses for each concentration. The linear regression analysis was performed  
171 by using the least squares method with the Excel analysis toolpak. This method was also  
172 used to calculate the slope and the intercept as well as their respective standard  
173 deviation.

174

175 The limit of detection (LOD) has been statistically determined from the calibration plot  
176 according to Eq. (1)

$$177 \quad LOD = kS_b/m \quad (1)$$

178 where  $k = 3$ ,  $S_b$  is the intercept standard deviation of the regression line and  $m$  is the  
179 slope of the linear calibration plot [46]. The limit of quantification (LOQ) was  
180 calculated with the same equation as for the detection limit; however, the k-value was  
181 taken to be 10.

182

## 183 **2.7 Speciation model**

184 The geochemical modelling program *Visual Minteq*, ver. 3.0 (using the standard  
185 databases) [47] was used to predict metal speciation in mineral water. The following  
186 inputs were provided: pH, temperature (25°C), and total concentrations for Ca, Na, K,  
187 Mg, carbonates, nitrates, sulfates, chlorides, Cu and Pb.

188

## 189 **3. Results and discussion**

### 190 **3.1 Electrochemical behaviour of catechol on SPCE**

191 The functionalization of the transducer is an important step in the development of an  
192 electrochemical sensor, as it will determine the performance of the electrodes in terms

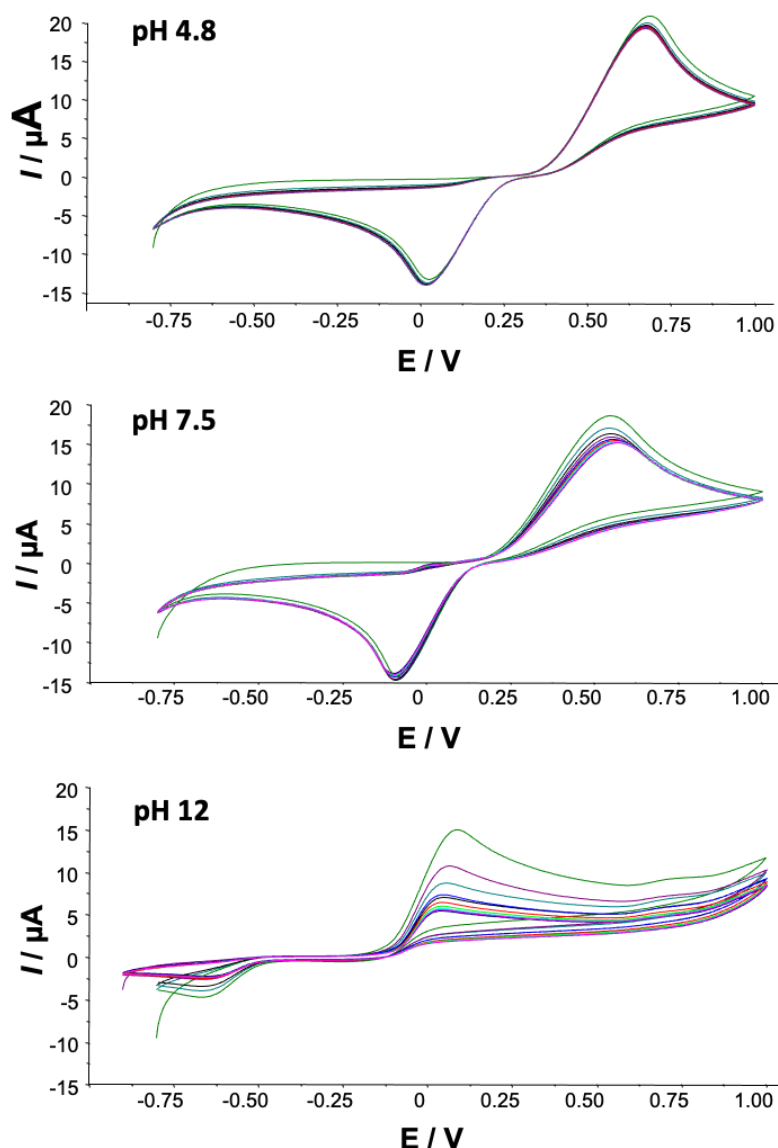
193 of sensitivity and stability over time. Our objective was first to optimise the  
194 electropolymerisation of catechol to obtain a stable and reproducible polycatechol film.  
195 Firstly, two types of electrodes were tested, SPCE and GCE. CV electropolymerisation  
196 of catechol showed that consecutive scans do not lead to a change in the anodic peak,  
197 suggesting that the polymer does not deposit on the GCE surface (Figure S2).  
198 Comparison of the electrode surfaces suggested that the rough surface of SPCE was  
199 more favourable for electropolymerisation than the smooth surface of GCE (Figure S3).  
200

### 201 3.1.1 Effect of pH during electropolymerisation

202 As expected, CV performed in a solution of catechol at different pH values shows that  
203 redox processes are pH dependant (Figure 1). Whatever the pH, the first potential scan  
204 shows an anodic peak related to the oxidation of catechol to o-benzoquinone and a  
205 corresponding cathodic peak related to the reduction of o-benzoquinone to catechol.  
206 This redox process involves the transfer of two electrons and two protons [48, 49]. The  
207 following scans show a different behaviour depending on the pH. At acidic pH, the  
208 subsequent scans lead to a slight decrease of the anodic peak (5%) coupled with the  
209 appearance of a second oxidation peak at 0.21V, whose intensity increases with the  
210 cycles, suggesting the formation of a redox-active polymer film on the electrode surface  
211 [50]. This behaviour appears much more pronounced at neutral pH with the appearance  
212 of a second oxidation peak at 0.01V and a decrease in the catechol oxidation peak by  
213 22% after 10 scans. The highest pH leads to a marked decrease in peak height (64%)  
214 with the appearance of a second oxidation peak at 0.72V suggesting a rapid  
215 dimerisation process in solution, leading to the depletion of catechol [48].

216

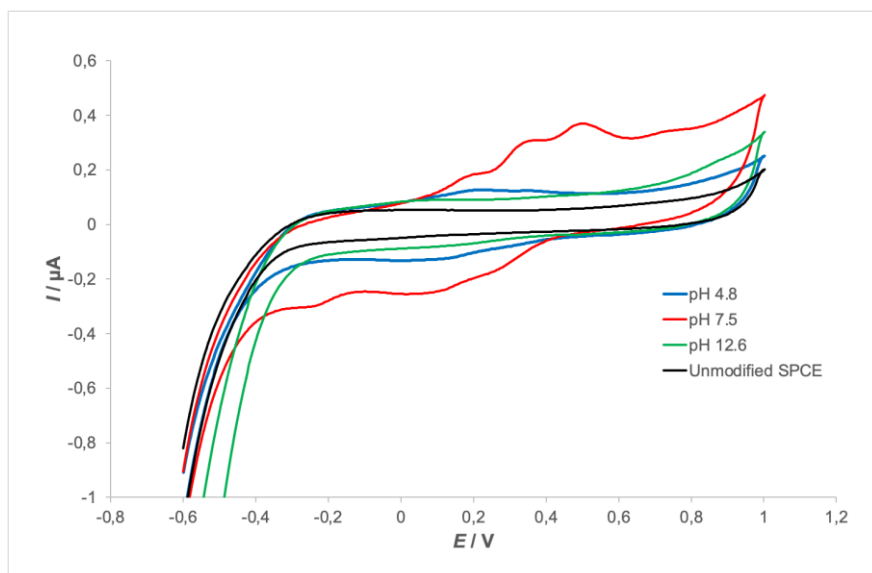
217



218 **Figure 1.** Electropolymerization of  $0.5 \text{ mmol L}^{-1}$  of catechol at different pH 4.8, 7.5 and 12.6. Cyclic  
 219 voltammetry from -0.8 to 1V at  $200 \text{ mV s}^{-1}$ . First scan is represented in green and last scan in purple.  
 220

221  
 222 In order to check the deposition of the polycatechol film, CV were performed in acetate  
 223 buffer solution without catechol. **Erreur ! Source du renvoi introuvable.** confirms that  
 224 the polymerisation pH leads to different mechanisms of electrodeposition. An acidic pH  
 225 allows the formation of a slightly electroactive film with only one redox couple. A basic  
 226 pH does not lead to any significant modification of the electrode, compared to an  
 227 unmodified electrode, which confirms the absence of polymerisation at this pH. On the  
 228 contrary, neutral pH seems to be the most favourable for the formation of an  
 229 electroactive polymer on the electrode surface with 3 redox couples observed in the  
 230 blank solution, immediately after electropolymerisation [50]. These observations are in  
 231 agreement with those of Marczewska (2013) who showed that the polymerisation  
 232 process works from weakly acidic medium (pH 5.4) to weakly alkaline medium (pH

233 9.2) [51]. Moreover, it is interesting to note that air drying of the modified electrodes  
234 leads to a strong decrease in these redox peaks (not shown) suggesting an irreversible  
235 oxidation of the polymer by oxygen in the air. For this reason, the modified electrodes  
236 were then air-dried for 24 hours before use.  
237



238  
239 **Figure 2.** Cyclic voltammograms of polymerized SPCE at different pH in a blank solution (acetate buffer,  
240 0.1 M, pH 4.8). Scan rate: 200 mV s<sup>-1</sup>.  
241

242 The proposed mechanism to explain the formation of an electroactive film on the  
243 electrode is the formation of a polymer *via* the coupling of mesomeric structures of  
244 phenoxy radical [52, 53]. Ortho-semiquinones, formed during the reduction steps from  
245 orthoquinones, are highly reactive species capable of reacting to form higher oligomers  
246 resulting in film deposition. When two of these ortho-semiquinones are sufficiently  
247 close, they undergo aryl-aryl coupling and progressive film deposition by  
248 polymerisation [54].

249 We can therefore conclude that the polymerisation process is initiated by the production  
250 of free radicals following the electrochemical oxidation of catechol to benzoquinone  
251 and its subsequent reduction to ortho-semiquinone (Figure S4). Once this radical  
252 initiator is formed, it attacks another monomer to initiate a polymer chain. Redox cycles  
253 allow the chain to propagate. Termination occurs during air drying, with oxygen acting  
254 as a polymerisation inhibitor.

255 The acidity dissociation constants ( $pK_a$ ) for its hydroxyl groups are both above 7:  $pK_{a1}$   
256 = 8.83 and  $pK_{a2}$  = 13.07 [55]. Changing the pH of the catechol solution leads to a  
257 change in and the dissociated forms and their concentration. Thus, at pH 7.5, the

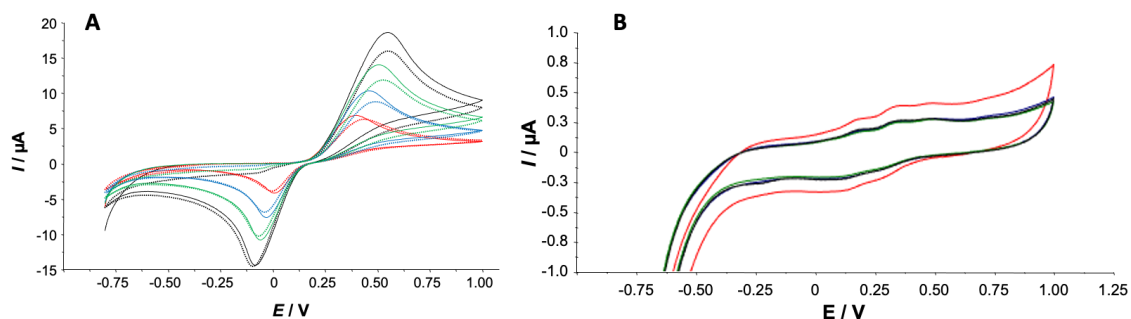
258 monoanion starts to form (between 2 and 4% depending on the  $pK_a$  value) whereas at  
259 pH 12, the catechol is in anionic form only. At higher pH, Pourghobadi *et al* proposes  
260 an alternative mechanism based on anionic or dianionic forms of catechol as  
261 nucleophiles that would rapidly add to the electrochemically generated o-benzoquinone,  
262 the rate of the dimerisation reaction increasing with pH [56].  
263 As our objective was to optimize and control the deposition of the film catechol on the  
264 surface of the working electrode, a pH of 7.5 was chosen for catechol  
265 electropolymerisation.

266

### 267 3.1.2 Effect of scan rate during electropolymerisation

268 Figure 3A shows the first and 10<sup>th</sup> scan obtained during electropolymerisation with  
269 different scan rates from 20 (red line) to 200  $\text{mV s}^{-1}$  (black line) in a phosphate buffer  
270 solution (0.1 M, pH 7.5) containing 0.5  $\text{mmol L}^{-1}$  of catechol. Increasing the scan rate  
271 induces an increase in peak height (x2.5), and in  $\Delta E_p$  (from 0.38 to 0.61V). The effect of  
272 scan rate on the properties of the polymer film was then studied in an acetate buffer  
273 solution at pH 4.6 (Figure 3B). Regardless of the scan rate, the polymerization of  
274 catechol leads to a film with 3 redox reactions (3 redox peaks). The lowest scan rate  
275 results in the highest capacitive current, while the other 3 scan rates give exactly the  
276 same voltammogram (Figure 3B). The slower the potential scan rate, the longer the life  
277 time of the semi-quinone radicals and the higher the probability of depositing thicker  
278 films with larger oligomers [54]. On the contrary, a high scan rate (200  $\text{mV s}^{-1}$ ) allows  
279 linear polymer growth due to a conductive and/or porous polymer matrix [57].  
280 Therefore, a scan rate of 200  $\text{mV s}^{-1}$  was chosen for the next experiments.

281



282

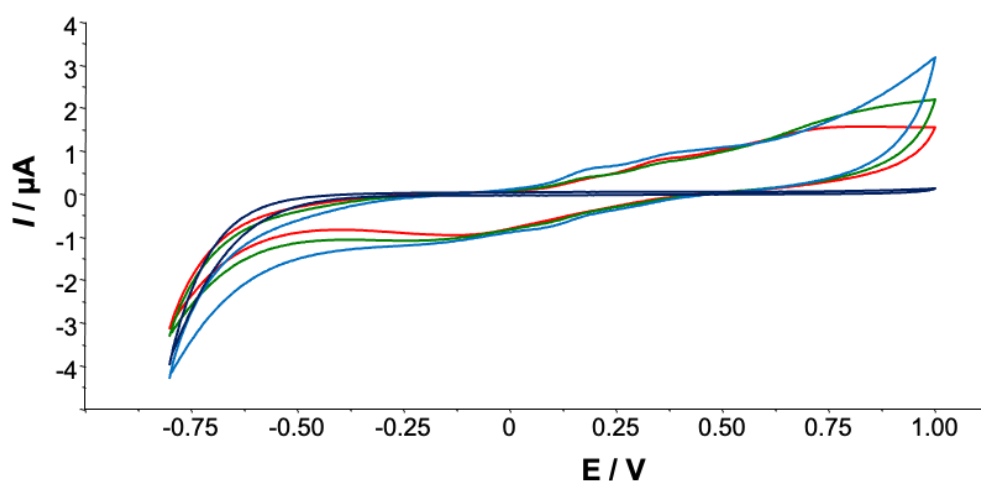
283 **Figure 3.** CV of polymerized SPCE at different scan rates: red line: 20  $\text{mV s}^{-1}$ , blue line: 50  $\text{mV s}^{-1}$ , green  
284 line: 100  $\text{mV s}^{-1}$  and black line: 200  $\text{mV s}^{-1}$  in a 0.5  $\text{mmol L}^{-1}$  catechol solution (pH 7.5). **A** - first scan  
285 (solid line) and last scan (dotted line) of catechol film polymerization; **B** - CV in a 0.1 M acetate buffer  
286 solution (pH 4.8; scan rate: 200  $\text{mV s}^{-1}$ ).

287

### 288 3.1.3 Effect of scan number during electropolymerisation

289 Figure 4 shows the effect of the number of scans on the properties of the polymer film.  
290 The polymer films obtained after 10, 20 or 50 scans show similar behaviour.  
291 Voltammograms obtained in acetate buffer solution show that the capacitive current  
292 does not increase with the number of polymerisation cycles suggesting that the polymer  
293 is porous and/or conductive (Figure 4). According to Almeida *et al.*, the mass growth  
294 profile of polycatechol is approximately linear during the 50 polymerization cycles due  
295 to the continuous oxidation of catechol at the electrode surface [38]. Consequently, an  
296 electropolymerisation of catechol based on 50 CV was retained for the following  
297 experiments which aim to detect trace metals in freshwater samples.

298



299

300 **Figure 4.** CV of polymerized SPCE from different scan number (black line: unmodified SPCE, red line:  
301 10 scans, green line: 20 scans and blue line: 50 scans) in a blank solution (acetate buffer 0.1 M at pH 4.8;  
302 scan rate: 200 mV s<sup>-1</sup>).

303

## 304 **3.2 Electrochemical detection of Cu and Pb by stripping** 305 **chronopotentiometry**

### 306 3.2.1 Optimization of the stripping current

307 By varying the applied stripping current, the stripping time regime can be varied from  
308 semi-infinite linear diffusion conditions ( $I\tau^{1/2}$  constant) to conditions approaching  
309 complete depletion ( $I\tau$  constant) [44]. These fully depletion conditions are particularly  
310 attractive for *in situ* application in samples such as freshwater as they lead to greater  
311 sensitivity, and are not affected by adsorption effects [58]. They allow measurements to  
312 be made without removing oxygen from the solution [11]. These conditions are  
313 therefore suitable for *in situ* analyses of Cu and Pb. The influence of the stripping

314 current on the Cu signal was evaluated in order to establish the experimental conditions  
315 under which the complete depletion regime was reached. Figure S5 shows that for the  
316 values of  $I_s$  between 1 and 20  $\mu\text{A}$ , the complete depletion regime  $I\tau$  (constant) is  
317 reached from stripping currents between 5 and 20  $\mu\text{A}$ . Regardless of the value of  $I_s$ ,  
318 plotting  $I\tau^{1/2}$  as a function of  $I_s$  never resulted in a plateau. As a result, a stripping  
319 current of 10  $\mu\text{A}$  was chosen for the following experiments.

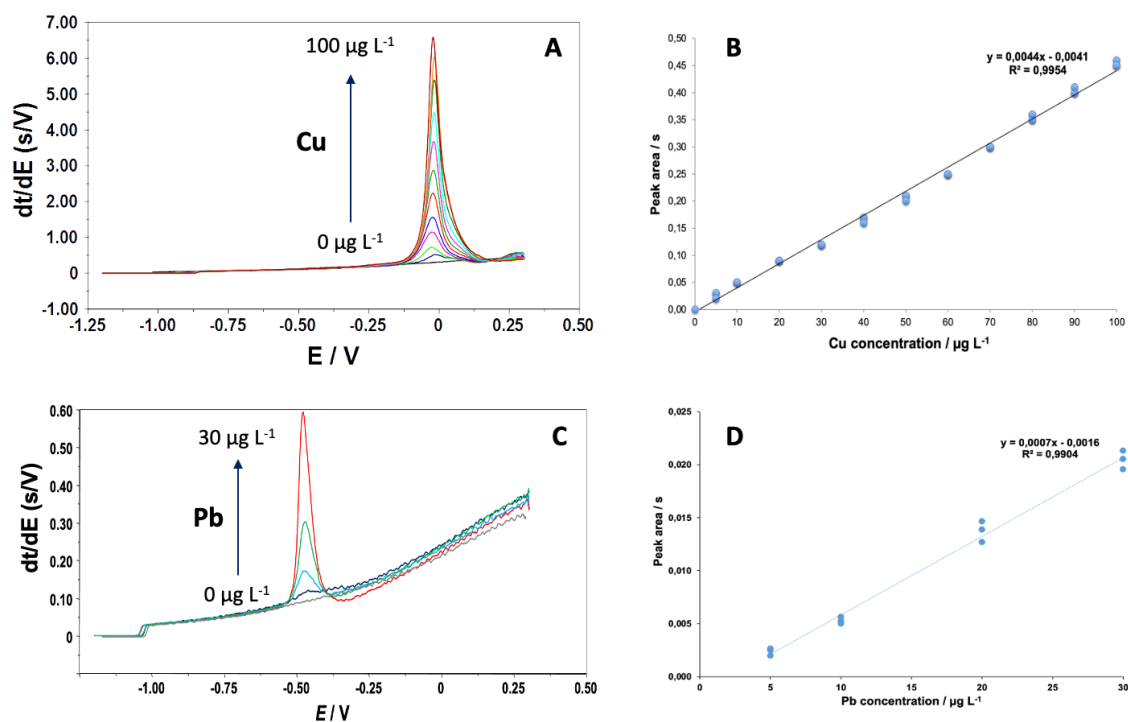
320

### 321 3.2.2 Analytical performance of the modified SPCE for metals 322 determination

323 The calibration plot for Cu in a sodium acetate solution buffered to pH 4.6 shows that a  
324 sensitivity of  $0.0044 \pm 0.0005 \text{ s}/\mu\text{g L}^{-1}$  and a linearity of  $5 \mu\text{g L}^{-1}$  to  $100 \mu\text{g L}^{-1}$  can be  
325 obtained, which corresponds to working conditions well suited to the detection of Cu in  
326 drinking water (Figure 5A and 6B). A LOD of  $2 \mu\text{g L}^{-1}$  and a LOQ of  $7 \mu\text{g L}^{-1}$  were  
327 obtained for a preconcentration time of 60 s. Similar results were obtained for Pb with a  
328 LOD of  $2 \mu\text{g L}^{-1}$  and a LOQ of  $6 \mu\text{g L}^{-1}$ , although this sensor appeared less sensitive for  
329 Pb with a slope of  $0.00075 \pm 0.00002 \text{ s}/\mu\text{g L}^{-1}$  (Figure 5C and 6D). These results are  
330 promising for monitoring purposes as a measurement time of 60 s allows the detection  
331 of concentrations in the  $\mu\text{g/L}$  range which is in perfect agreement with the values set by  
332 legislation.

333 However, these values could be improved by increasing the deposition time since the  
334 longer the deposition time, the higher the amount of analyte is available at the electrode  
335 during the analysis (Figure S6). Thus, for Pb, increasing the electrodeposition time from  
336 60s to 300 s resulted in a calibration line between 100 and 500  $\text{ng L}^{-1}$  with a LOD of 63  
337  $\text{ng L}^{-1}$  and a LOQ of 92  $\text{ng L}^{-1}$  (Figure S7). These results are slightly higher than those  
338 of Poudel et al for Pb who obtained a LOD of 3.7  $\text{ng/L}$  after a waiting time (extraction  
339 and reduction) of 1060 s which does not allow continuous *in situ* monitoring [59].  
340 Higher concentrations can also be detected by using an electrochemical method less  
341 sensitive such as linear scan voltammetry which allows the detection of Cu up to 5  $\text{mg}$   
342  $\text{L}^{-1}$  (Figure S8). These results show the power of the electrochemistry to detect a wide  
343 range of concentrations from  $\text{ng L}^{-1}$  to  $\text{mg L}^{-1}$ , only by modifying the electrodeposition  
344 time and/or the electrochemical method.

345



346

347 **Figure 5.** Stripping Chronopotentiometric response of Cu (A) and Pb (C) and calibration plot of Cu (B)  
 348 and Pb (D) obtained with a modified SPCE in acetate buffer 0.1 mol L<sup>-1</sup>. Analysis conditions:  
 349 electrodeposition: 60 s at -1.2 V with stirring, equilibration time 10 s at -1.2 V without stirring, stripping  
 350 current  $I_s = 10 \mu\text{A}$  without stirring.

351

### 352 3.2.3 Repeatability and reproducibility

353 Figure S9 shows Cu signal obtained for 8 modified SPCEs coming from the same  
 354 screen-printing plate (Figure S9A) and for 8 modified SPCEs from 8 different screen-  
 355 printing plates (Figure S9B). No significant difference was observed between the  
 356 different modified electrodes, where a Cu concentration of 20  $\mu\text{g L}^{-1}$  led to a peak area  
 357 of  $0.064 \text{ s} \pm 0.004 \text{ s}$  for electrodes from the same plate and of  $0.072 \text{ s} \pm 0.005 \text{ s}$  for  
 358 electrodes from different plates. This result underlines the robustness of the sensor  
 359 construction, from serigraphy to modification of the surface, which is promising for the  
 360 development of a field sensor.

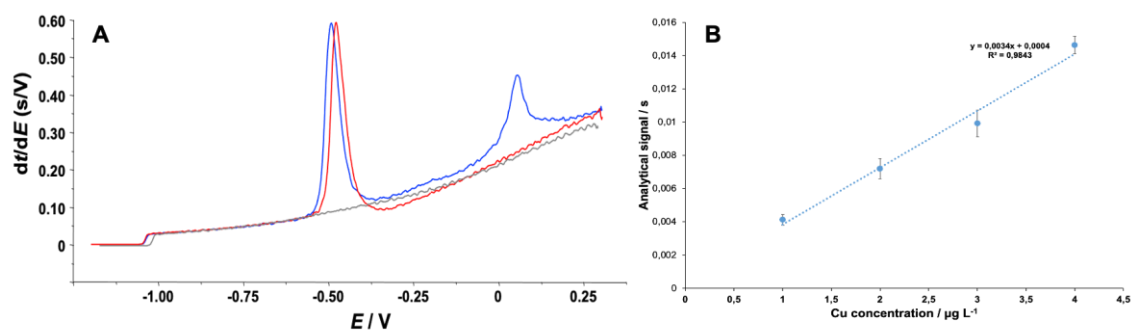
361

### 362 3.2.4 Simultaneous detection of Cu and Pb

363 Figure 6A shows the Pb signal obtained that simultaneous detection of Pb and Cu is not  
 364 a problem as these metals don't have the same redox potential with -0.48 V for Pb and  
 365 +0.06 V for Cu. The addition of Cu in the solution doesn't change the Pb signal which  
 366 suggests that there is no interference. However, Figure 6B shows that the calibration  
 367 plot obtained for Cu concentrations from 1 to 4  $\mu\text{g L}^{-1}$ , in the presence of 30  $\mu\text{g L}^{-1}$  of

368 Pb gives a slope of  $0.0034 \pm 0.0002$  s/ $\mu\text{g L}^{-1}$  which is slightly lower than that obtained  
369 in the absence of Pb ( $0.0044 \pm 0.0005$  s/ $\mu\text{g L}^{-1}$ ). On the contrary, when the Cu/Pb  
370 concentration ratios are reversed, the Cu signal is little affected by the presence of Pb  
371 (Figure S10). All these results mean that in the case of a multi-metal contamination, a  
372 calibration taking into account the different metals in solution will be necessary to  
373 obtain an accurate value.

374



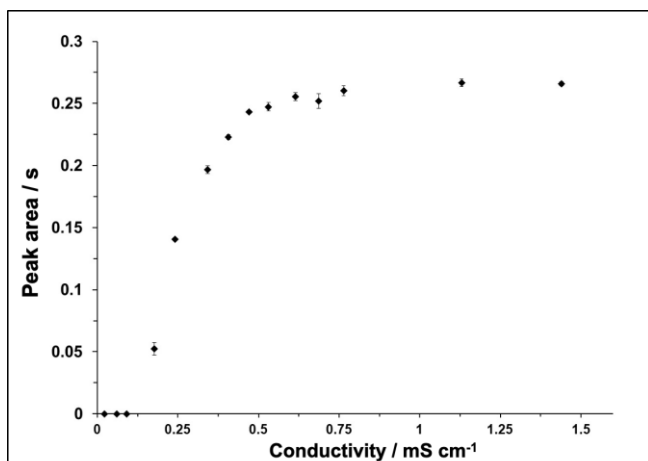
375  
376  
377  
378  
379

**Figure 6.** **A** - Analytical signal of Pb ( $30 \mu\text{g L}^{-1}$ ) without or with Cu ( $4 \mu\text{g L}^{-1}$ ); **B** - Calibration plot of Cu from 1 to 4  $\mu\text{g L}^{-1}$  in presence of Pb at  $30 \mu\text{g L}^{-1}$ . Analysis conditions: acetate buffer  $0.1 \text{ mol L}^{-1}$  at pH 4.6, deposition at  $-1.2 \text{ V}$  for 60 s, stripping current  $I_s = 10 \mu\text{A}$ .

### 380 3.2.5 Effect of the conductivity of the sample

381 Conductivity is also an important parameter to take into account when analysing natural  
382 freshwater samples because this parameter can strongly change from one sample to  
383 another. Parat *et al* analysed different natural freshwaters from some rivers in the  
384 Pyrenees (France) and found conductivities ranging from 78 to  $211 \mu\text{S cm}^{-1}$  [13] while  
385 Platikanov *et al* who collected tap waters from different locations in Catalonia (Spain),  
386 found conductivities ranging from  $82.3 \mu\text{S cm}^{-1}$  to  $2417 \mu\text{S cm}^{-1}$  [60]. Therefore, the  
387 effects of solution conductivity on Cu signal were studied in ultrapure water doped with  
388 Cu at  $50 \mu\text{g L}^{-1}$  in which successive additions of acetate ( $1 \text{ mol L}^{-1}$ ) were made. Figure  
389 7 shows the variation of the signal (peak area) obtained for Cu at different  
390 conductivities, with a plateau from a conductivity of  $470 \mu\text{S cm}^{-1}$ , a value close to those  
391 found in most natural freshwaters.

392



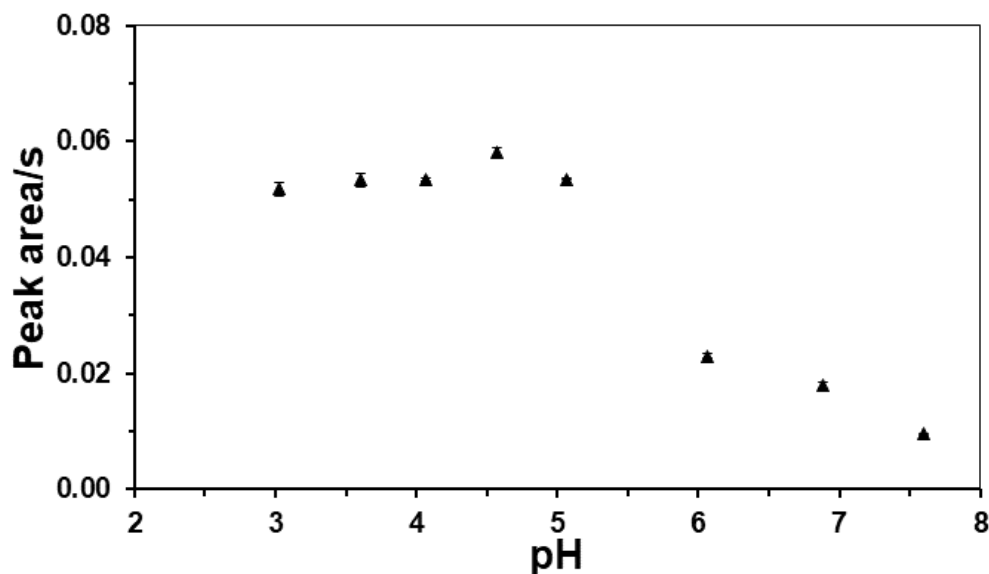
393

394 **Figure 7.** Effect of conductivity on Cu signal (Cu concentration = 50  $\mu\text{g L}^{-1}$ ) obtained with a modified  
 395 SPCE. Analysis conditions: electrodeposition: 60 s at -1.2 V with stirring, equilibration time 10 s at -1.2  
 396 V without stirring, stripping current  $I_s = 10 \mu\text{A}$  without stirring.

397

### 398 3.2.6 Effect of pH on water samples

399 The effect of pH on the response of the modified SPCE in the presence of Cu was  
 400 studied over a pH range of 3 to 7.6. The pH was adjusted to the different values by  
 401 adding acetic acid to mineral water. The signal shows a stable peak area between pH 3  
 402 and 5 (Figure 8). At higher pH, a sharp decrease in signal is observed from 57% at pH 6  
 403 to 82% at pH 7.6. This behaviour can be due to the inorganic compounds (bicarbonates,  
 404 sulphates and nitrates) present in the solution, and capable of forming Cu complexes,  
 405 which are not electrolabile. The Visual MINTEQ speciation model confirms that the  
 406 proportion of free Cu in mineral water depends on pH with only 3.8 % of free Cu at pH  
 407 7.6. At this pH, carbonates appear as the main compound complexing Cu (90%) and  
 408 blocking its electrochemical detection (Table 1). Acidification of the sample with acetic  
 409 acid from pH 7.6 to 4 changes the Cu speciation leading to 69 % of free Cu and about  
 410 27% of Cu-acetate complexes that are electrolabile. Lead shows the same behaviour  
 411 with about 88% of Pb-carbonate complexes at pH 7.6 and only 5.6 % of free Pb. The  
 412 acidification of the solution leads to a modification of the speciation with about 95% of  
 413 labile Pb (Table S1). This means that the determination of the total concentration of Cu  
 414 and Pb will require a prior acidification of the solution at pH 5 or less to dissociate Cu  
 415 and Pb carbonate complexes present in solution.



416

417 **Figure 8.** Variation of Cu signal according to the pH obtained with a catechol modified SPCE in a  
 418 mineral water. Analysis conditions: Cu concentration:  $20 \mu\text{g L}^{-1}$ , electrodeposition: 60 s at -1.2 V with  
 419 stirring, equilibration time 10 s at -1.2 V without stirring, stripping current  $I_s = 10 \mu\text{A}$  without stirring.  
 420

420

421 **Table 1.** Speciation of Cu (in %) computed from Visual Minteq 3.0 in mineral water at pH 7.6 and  
 422 acidified with acetic acid from pH 7 to 4

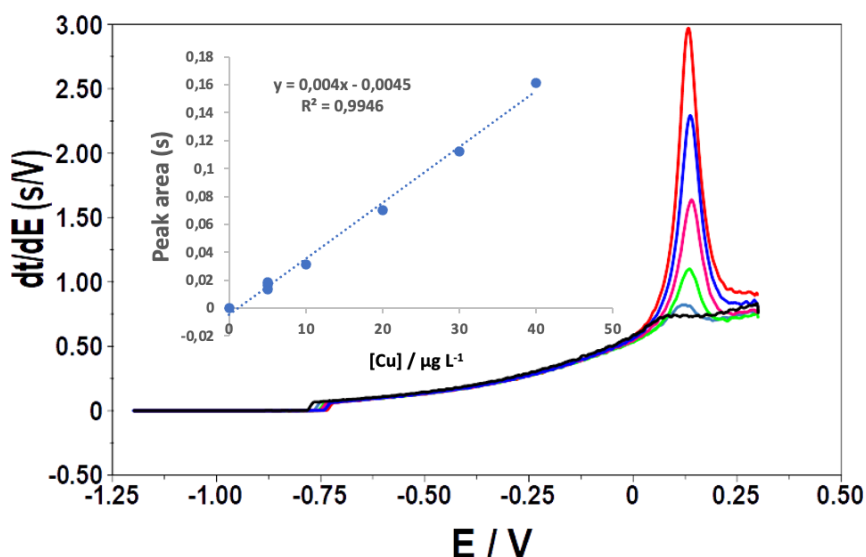
	pH 7.6	pH 7	pH 6	pH 5	pH 4.6	pH 4
$\text{Cu}^{2+}$	3.8	14.9	62.7	69.4	69.1	68.9
$\text{CuOH}^+$	3.7	3.6	1.5	0.2	0.1	
$\text{Cu}(\text{OH})_2$ (aq)	0.2	0.1				
$\text{CuCl}^+$			0.1	0.1	0.1	0.1
$\text{CuSO}_4$ (aq)	0.1	0.6	2.3	2.6	2.6	2.5
$\text{CuCO}_3$ (aq)	89.6	77.7	13.1	0.2		
$\text{CuHCO}_3^+$	0.6	1.9	3.3	0.5	0.2	0.1
$\text{Cu-Acetate}^+$	2.0	0.4	16.5	25.9	26.7	27.2
$\text{Cu-(Acetate)}_2$ (aq)		0.8	0.5	1.1	1.2	1.2

423

### 424 3.3 Analysis of acidified mineral water by using modified SPCE

425 A calibration plot was carried out in a mineral water sample previously acidified with  
 426 acetic acid to dissociate all Cu-complexes (Figure 9) and compared to that obtained in  
 427 acetate solution. The deposition time and SCP parameters were the same as those used  
 428 previously. A slope of  $0.0041 \text{ s}/\mu\text{g L}^{-1}$  was obtained in acidified mineral water which is  
 429 similar to that obtained in  $0.1 \text{ mol L}^{-1}$  acetate buffer ( $0.0044 \pm 0.0005 \text{ s}/\mu\text{g L}^{-1}$ ) showing  
 430 that no interfering effect occurs in a solution such as a mineral water.

431



432 **Figure 9.** Stripping chronopotentiometric response and Cu calibration plot obtained with modified SPE  
 433 sensor in the presence of different copper concentrations in acidified mineral water (pH 4). Analysis  
 434 conditions: electrodeposition: 60 s at -1.2 V with stirring, equilibration time 10 s at -1.2 V without  
 435 stirring, stripping current  $I_s = 10 \mu\text{A}$  without stirring.  
 436  
 437

#### 438 **4. Conclusion**

439 A new electrochemical sensor has been developed for the detection of Cu and Pb in  
 440 acidified drinking water. For this purpose, a screen-printed carbon electrode was  
 441 modified by a polycatechol film. Different parameters were studied to obtain a  
 442 homogeneous and stable film, as the effect of pH, the scan rate and the number of  
 443 electropolymerisation scans. Optimisation of the polymerisation conditions resulted in a  
 444 highly reproducible electrochemical platform indicating a simple and robust method of  
 445 sensor fabrication.

446 High performance was achieved using stripping chronopotentiometry (SCP) to detect Cu  
 447 and Pb in acetate buffer at pH 4.6. We showed the power of the electrochemistry to  
 448 detect a wide range of concentrations from  $\text{ng L}^{-1}$  to  $\text{mg L}^{-1}$  with the same working  
 449 electrode, only by modifying the electrodeposition time and/or the electrochemical  
 450 method (SCP or LSV).

451 From a more general point of view, compared to previous studies aimed at developing  
 452 electrochemical sensors for trace metal detection in drinking water, we demonstrate for  
 453 the first time an efficient and sensitive electrode based on a polycatechol film. This  
 454 preparation method is interesting because it can easily replace the deposition of  
 455 expensive, toxic (mercury film) and sometimes complicated synthetic molecules like  
 456 cyclodextrins and calixarene used for detection of trace metal such as Cu. The analytical  
 457 performances obtained, namely a good reproducibility, a good repeatability and a

458 sensitivity range in agreement with the concentrations found in acidified mineral water  
459 for Pb and Cu for measurement time between 60 s and 300s, make this modified SPCE  
460 an ideal candidate for industrialisation for monitoring the aquatic environment.  
461 Research is underway to develop an industrial sensor where the three electrodes  
462 (working, auxiliary and reference) would be combined on a single sensor.

463

## 464 **Acknowledgments**

465 We would like to acknowledge the financial support of our collaborator “SYCLOPE  
466 ELECTRONIQUE” for the industrial project “GREEN SENSOR”.

467

## 468 **References**

- 469 [1] L. Chang, J.H.W. Lee, Y.S. Fung, Prediction of lead leaching from galvanic  
470 corrosion of lead-containing components in copper pipe drinking water supply systems,  
471 *J Hazard Mater* 436 (2022) 129169.
- 472 [2] WHO, Guidelines for drinking-water quality: fourth edition incorporating the first  
473 and second addenda., World Health Organization (WHO), Geneva, 2022, p. 614.
- 474 [3] WHO, Copper in Drinking-water, Guidelines for Drinking-water Quality, World  
475 Health Organization (WHO), 2004, p. 31.
- 476 [4] Directive 2020/2184/EU of the european parliament and of the council of 16  
477 December 2020 on the quality of water intended for human consumption, Official  
478 Journal of the European Union, 2020, p. 62.
- 479 [5] WHO, Lead in drinking-water: Health risks, monitoring and corrective actions,  
480 World Health Organization (WHO), 2022, p. 26.
- 481 [6] P.M. Madhu, R.S. Sadagopan, Effect of Heavy Metals on Growth and Development  
482 of Cultivated Plants with Reference to Cadmium, Chromium and Lead – A Review,  
483 *Journal of Stress Physiology & Biochemistry* 16 (2020) 84-102.
- 484 [7] S. Hussain, T. Sultana, S. Sultana, B. Hussain, S. Mahboob, K.A. Al-Ghanim, M.N.  
485 Riaz, Seasonal monitoring of River through heavy metal bioaccumulation and  
486 histopathological alterations in selected fish organs, *Journal of King Saud University -*  
487 *Science* 33(8) (2021).
- 488 [8] M. Cuartero, Electrochemical sensors for in-situ measurement of ions in seawater,  
489 *Sensors and Actuators B: Chemical* 334 (2021) 129635.
- 490 [9] S. Betelu, C. Parat, N. Petrucciani, A. Castetbon, L. Authier, M. Potin-Gautier,  
491 Semicontinuous monitoring of cadmium and lead with a screen-printed sensor modified  
492 by a membrane, *Electroanalysis* 19(2-3) (2007) 399-402.
- 493 [10] C. Parat, L. Authier, S. Betelu, N. Petrucciani, M. Potin-Gautier, Determination of  
494 labile cadmium using a screen-printed electrode modified by a microwell,  
495 *Electroanalysis* 19 (2007) 403-406.
- 496 [11] C. Parat, A. Schneider, A. Castetbon, M. Potin-Gautier, Determination of trace  
497 metal speciation parameters by using screen-printed electrodes in stripping  
498 chronopotentiometry without deaerating, *Analytica Chimica Acta* 688 (2011) 156-162.
- 499 [12] O. Zaouak, L. Authier, C. Cugnet, A. Castetbon, M. Potin-Gautier,  
500 Electroanalytical device for cadmium speciation in waters. Part 1: Development and

501 characterization of a reliable screen-printed sensor, *Electroanalysis* 22 (2010) 1151-  
502 1158.

503 [13] C. Parat, L. Authier, A. Castetbon, D. Aguilar, E. Companys, J. Puy, J. Galceran,  
504 M. Potin-Gautier, Free Zn<sup>2+</sup> determination in natural freshwater of the Pyrenees:  
505 towards on-site measurements with AGNES, *Environmental Chemistry* 12 (2015) 329-  
506 337.

507 [14] H. Xiang, Q. Cai, Y. Li, Z. Zhang, L. Cao, K. Li, H. Yang, Sensors Applied for the  
508 Detection of Pesticides and Heavy Metals in Freshwaters, *Journal of Sensors* 2020  
509 (2020) 1-22.

510 [15] O.D. Renedo, M. Julia Arcos Martinez, A novel method for the anodic stripping  
511 voltammetry determination of Sb(III) using silver nanoparticle-modified screen-printed  
512 electrodes, *Electrochemistry Communications* 9(4) (2007) 820-826.

513 [16] M. Li, Y.-T. Li, D.-W. Li, Y.-T. Long, Recent developments and applications of  
514 screen-printed electrodes in environmental assays - A review, *Analytica Chimica Acta*  
515 734(0) (2012) 31-44.

516 [17] X. Liu, Y. Yao, Y. Ying, J. Ping, Recent advances in nanomaterial-enabled screen-  
517 printed electrochemical sensors for heavy metal detection, *TrAC Trends in Analytical*  
518 *Chemistry* 115 (2019) 187-202.

519 [18] A. García-Miranda Ferrari, P. Carrington, S.J. Rowley-Neale, C.E. Banks, Recent  
520 advances in portable heavy metal electrochemical sensing platforms, *Environmental*  
521 *Science: Water Research & Technology* 6(10) (2020) 2676-2690.

522 [19] J.-Y. Choi, K. Seo, S.-R. Cho, J.-R. Oh, S.-H. Kahng, J. Park, Screen-printed  
523 anodic stripping voltammetric sensor containing HgO for heavy metal analysis,  
524 *Analytica Chimica Acta* 443(2) (2001) 241-247.

525 [20] K.C. Honeychurch, J.P. Hart, Screen-printed electrochemical sensors for  
526 monitoring metal pollutants, *TrAC Trends in Analytical Chemistry* 22(7) (2003) 456-  
527 469.

528 [21] C. Parat, S. Betelu, L. Authier, M. Potin-Gautier, Determination of labile trace  
529 metals with screen-printed electrode modified by a crown-ether based membrane,  
530 *Analytica Chimica Acta* 573-574 (2006) 14-19.

531 [22] W. Wang, Stripping Analysis at Bismuth Electrodes: A Review, *Electroanalysis*  
532 17(15-16) (2005) 1341-1346.

533 [23] I. Svancara, L. Baldrianová, E. Tesarová, S.B. Hocevar, A.A. Elsuccary, A.  
534 Economou, S. Sotiropoulos, B. Ogorevc, K. Vytras, Recent Advances in Anodic  
535 Stripping Voltammetry with Bismuth-Modified Carbon Paste Electrodes,  
536 *Electroanalysis* 18(2) (2006) 177-185.

537 [24] A. Sanchez-Calvo, M.C. Blanco-Lopez, A. Costa-Garcia, Paper-Based Working  
538 Electrodes Coated with Mercury or Bismuth Films for Heavy Metals Determination,  
539 *Biosensors (Basel)* 10 (2020) bios10050052.

540 [25] S. Laschi, I. Palchetti, M. Mascini, Gold-based screen-printed sensor for detection  
541 of trace lead, *Sensors and Actuators B: Chemical* 114(1) (2006) 460-465.

542 [26] P. Salaün, B. Planer-Friedrich, C.M.G. van den Berg, Inorganic arsenic speciation  
543 in water and seawater by anodic stripping voltammetry with a gold microelectrode,  
544 *Analytica Chimica Acta* 585(2) (2007) 312-322.

545 [27] R.D. Riso, M. Waeles, P. Monbet, C.J. Chaumery, Measurements of trace  
546 concentrations of mercury in sea water by stripping chronopotentiometry with gold disk  
547 electrode: influence of copper, *Analytica Chimica Acta* 410(1-2) (2000) 97-105.

548 [28] Z. Ait-Touchente, S. Falah, E. Scavetta, M.M. Chehimi, R. Touzani, D. Tonelli, A.  
549 Taleb, Different Electrochemical Sensor Designs Based on Diazonium Salts and Gold  
550 Nanoparticles for Pico Molar Detection of Metals, *Molecules* 25(17) (2020).

- 551 [29] M.B. Gumpu, S. Sethuraman, U.M. Krishnan, J.B.B. Rayappan, A review on  
552 detection of heavy metal ions in water – An electrochemical approach, *Sensors and*  
553 *Actuators B: Chemical* 213(0) (2015) 515-533.
- 554 [30] L. Cui, J. Wu, H. Ju, Electrochemical sensing of heavy metal ions with inorganic,  
555 organic and bio-materials, *Biosensors and Bioelectronics* 63(0) (2015) 276-286.
- 556 [31] O. Kanoun, T. Lazarevic-Pasti, I. Pasti, S. Nasraoui, M. Talbi, A. Brahem, A.  
557 Adiraju, E. Sheremet, R.D. Rodriguez, M. Ben Ali, A. Al-Hamry, A Review of  
558 Nanocomposite-Modified Electrochemical Sensors for Water Quality Monitoring,  
559 *Sensors (Basel)* 21(12) (2021) s21124131.
- 560 [32] D. Tyagi, H. Wang, W. Huang, L. Hu, Y. Tang, Z. Guo, Z. Ouyang, H. Zhang,  
561 Recent advances in two-dimensional-material-based sensing technology toward health  
562 and environmental monitoring applications, *Nanoscale* 12(6) (2020) 3535-3559.
- 563 [33] C. Kumunda, A.S. Adekunle, B.B. Mamba, N.W. Hlongwa, T.T.I. Nkambule,  
564 Electrochemical Detection of Environmental Pollutants Based on Graphene Derivatives:  
565 A Review, *Frontiers in Materials* 7 (2021) 616787.
- 566 [34] A.M. Sanjuán, J.A. Reglero Ruiz, F.C. García, J.M. García, Recent developments  
567 in sensing devices based on polymeric systems, *React Funct Polym* 133 (2018) 103-  
568 125.
- 569 [35] X. Zheng, S. Khaoulani, N. Ktari, M. Lo, A.M. Khalil, C. Zerrouki, N. Fourati,  
570 M.M. Chehimi, Towards Clean and Safe Water: A Review on the Emerging Role of  
571 Imprinted Polymer-Based Electrochemical Sensors, *Sensors (Basel)* 21(13) (2021).
- 572 [36] Y. Wang, A. Liu, Y. Han, T. Li, Sensors based on conductive polymers and their  
573 composites: a review, *Polymer International* 69 (2020) 7-17.
- 574 [37] E. Faure, C. Falentin-Daudré, C. Jérôme, J. Lyskawa, D. Fournier, P. Woisel, C.  
575 Detrembleur, Catechols as versatile platforms in polymer chemistry, *Progress in*  
576 *Polymer Science* 38(1) (2013) 236-270.
- 577 [38] L.C. Almeida, R.D. Correia, B. Palys, J.P. Correia, A.S. Viana, Comprehensive  
578 Study of the Electrochemical Growth and Physicochemical Properties of  
579 Polycatecholamines and Polycatechol, *Electrochimica Acta* (2021).
- 580 [39] V.T. Athavale, L.H. Prabhu, D.G. Vartak, Solution stability constants of some  
581 metal complexes of derivatives of catechol, *Journal of Inorganic and Nuclear Chemistry*  
582 28(5) (1966) 1237-1249.
- 583 [40] A.E. Martell, R.M. Smith, Critical stability constants: Other Organic Ligands,  
584 1977.
- 585 [41] V.M. Vorotyntsev, E.P. Kuznetsova, Y.I. Pyatnitskii, G.I. Golodets, Homogeneous  
586 catalytic oxidation of pyrocatechol in the presence of transition metal ions, *React Kinet*  
587 *Catal Lett* 13(4) (1980) 373-378.
- 588 [42] A. Bačinić, L.-M. Tumir, M. Mlakar, Electrochemical characterization of  
589 Cobalt(II)-Complexes involved in marine biogeochemical processes. I. Co(II)-4-  
590 nitrocatechol and Co(II)-Humate, *Electrochimica Acta* 337 (2020) 135797.
- 591 [43] S.B. Khoo, J. Zhu, Poly(catechol) Film Modified Glassy Carbon Electrode for  
592 Ultratrace Determination of Cerium(III) by Differential Pulse Anodic Stripping  
593 Voltammetry, *Electroanalysis* 11(8) (1999) 546-552.
- 594 [44] R.M. Town, H.P. van Leeuwen, Fundamental features of metal ion determination  
595 by stripping chronopotentiometry, *Journal of Electroanalytical Chemistry* 509(1) (2001)  
596 58-65.
- 597 [45] H.P. van Leeuwen, R.M. Town, Elementary features of depletive stripping  
598 chronopotentiometry, *Journal of Electroanalytical Chemistry* 535(1-2) (2002) 1-9.

- 599 [46] A. Shrivastava, V. Gupta, Methods for the determination of limit of detection and  
600 limit of quantitation of the analytical methods, *Chronicles of Young Scientists* 2(1)  
601 (2011).
- 602 [47] J.P. Gustafsson, Visual Minteq, version 3.0,  
603 <http://www2.lwr.kth.se/English/OurSoftware/vminteq/> (2010).
- 604 [48] M.D. Ryan, A. Yueh, W.-Y. Chen, The Electrochemical Oxidation of Substituted  
605 Catechols, *Journal of The Electrochemical Society* 127 (1980) 1489-1495.
- 606 [49] T. Palomäki, S. Chumillas, S. Sainio, V. Protopopova, M. Kauppila, J. Koskinen,  
607 V. Climent, J.M. Feliu, T. Laurila, Electrochemical reactions of catechol,  
608 methylcatechol and dopamine at tetrahedral amorphous carbon (ta-C) thin film  
609 electrodes, *Diamond and Related Materials* 59 (2015) 30-39.
- 610 [50] J. Bai, X. Bo, B. Qi, L. Guo, A Novel Polycatechol/Ordered Mesoporous Carbon  
611 Composite Film Modified Electrode and Its Electrocatalytic Application,  
612 *Electroanalysis* 22(15) (2010) 1750-1756.
- 613 [51] B. Marczewska, M. Przegaliński, Poly(catechol) electroactive film and its  
614 electrochemical properties, *Synthetic Metals* 182(0) (2013) 33-39.
- 615 [52] A. Raouafi, A. Rabti, N. Raouafi, A printed SWCNT electrode modified with  
616 polycatechol and lysozyme for capacitive detection of  $\alpha$ -lactalbumin, *Microchimica*  
617 *Acta* 184 (2017) 4351-4357.
- 618 [53] S. Kim, C. Silva, D.V. Evtuguin, J.A. Gamelas, A. Cavaco-Paulo,  
619 Polyoxometalate/laccase-mediated oxidative polymerization of catechol for textile  
620 dyeing, *Appl Microbiol Biotechnol* 89(4) (2011) 981-7.
- 621 [54] V. Ball, Electrodeposition of pyrocatechol based films: Influence of potential scan  
622 rate, pyrocatechol concentration and pH, *Colloids and Surfaces A: Physicochemical and*  
623 *Engineering Aspects* 518 (2017) 109-115.
- 624 [55] R. Romero, P.R. Salgado, C. Soto, D. Contreras, V. Melin, An Experimental  
625 Validated Computational Method for pKa Determination of Substituted 1,2-  
626 Dihydroxybenzenes, *Front Chem* 6 (2018) 208.
- 627 [56] R. Pourghobadi, D. Nematollahi, M.R. Baezzat, S. Alizadeh, H. Goljani,  
628 Electropolymerization of catechol on wireless graphite electrode. Unusual cathodic  
629 polycatechol formation, *Journal of Electroanalytical Chemistry* 866 (2020) 114180.
- 630 [57] L.C. Almeida, R.D. Correia, A. Marta, G. Squillaci, A. Morana, F. La Cara, J.P.  
631 Correia, A.S. Viana, Electrosynthesis of polydopamine films - tailored matrices for  
632 laccase-based biosensors, *Applied Surface Science* 480 (2019) 979-989.
- 633 [58] R.M. Town, H.P. van Leeuwen, Effects of adsorption in stripping  
634 chronopotentiometric metal speciation analysis, *Journal of Electroanalytical Chemistry*  
635 523(1-2) (2002) 1-15.
- 636 [59] A. Poudel, G.S. Shyam Sunder, A. Rohanifar, S. Adhikari, J.R. Kirchoff,  
637 Electrochemical determination of Pb<sup>2+</sup> and Cd<sup>2+</sup> with a poly(pyrrole-1-carboxylic  
638 acid) modified electrode, *Journal of Electroanalytical Chemistry* 911 (2022).
- 639 [60] S. Platikanov, D. Baquero, S. Gonzalez, J. Martin-Alonso, M. Paraira, J.L. Cortina,  
640 R. Tauler, Chemometric analysis for river water quality assessment at the intake of  
641 drinking water treatment plants, *Sci Total Environ* 667 (2019) 552-562.

642